Real-Time State Estimation Model for Converter Steelmaking

KASE Hiroto[*1] TOMIYAMA Shinji[*2] SATO Shingo[*3]

Abstract:

To achieve optimization and automation of the converter process, it is important to perform appropriate operations based on internal state information such as the composition of molten metal and slag. However, due to high temperature and explosive reaction inside the converter, it has been difficult to measure the internal state during processing. Therefore, JFE Steel has developed a model to estimate the internal state of the converter in real time, aiming to build a cyber-physical system of the converter. This model solves the conventional problems of decreased estimation accuracy caused by unknown disturbances and measurement errors, and achieves high-precision and real-time internal state estimation.

1. Introduction

The converter steelmaking is a refining process which is used for hot metal (molten pig iron) after tapping from the blast furnace and various pretreatment processes. In the converter process, sub-materials are added to the hot metal and high-pressure oxygen blowing is performed to control the contents of elements such as C, Si, Mn, P, etc. in the hot metal within the appropriate range and raise the temperature of the molten steel. Since real-time observation and dynamic control of the internal state of the converter are required to achieve high efficiency and low-cost converter operation, JFE Steel aims to achieve optimization and automation of converter operation by building a cyber-physical system (CPS) for the converter.

When applying CPS to the converter, observation of the internal state of the converter is extremely important. However, due to the high temperature, explosive reaction environment in the converter, it was difficult to measure the internal state during processing. Therefore, in the current operation, as shown in **Fig. 1**, the blowing conditions are determined based on the hot metal temperature obtained before the start of blowing, and the final operations are determined based on the C concentration in the hot metal and the temperature obtained by sampling the molten metal only one time after the start of blowing, that is, just before the end of blowing.

In operation as described above, the accuracy of composition and temperature controls of the hot metal is reduced by the effects of unknown external disturbances, etc. during blowing, which frequently cause the end-point composition and temperature to deviate from the target values. To solve this problem, JFE Steel

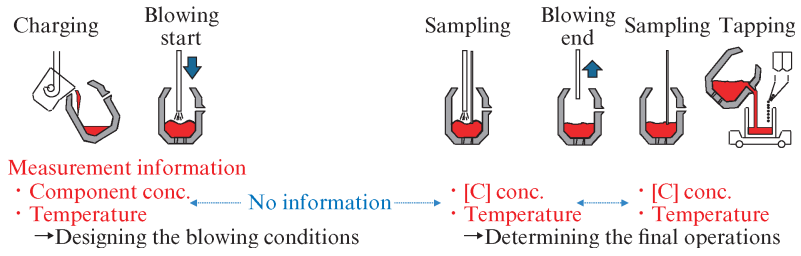

Fig. 1 Converter process

† Originally published in *JFE GIHO* No. 56 (Aug. 2025), p. 8−14

*1 Senior Researcher,
Cyber-Physical System Research & Development Dept.,
Steel Res. Lab., JFE Steel

*2 Senior Management Staff,
Intelligent Technology Development Dept.,
Digital Transformation Strategy Headquarter, JFE Steel

*3 Senior Management Researcher,
Cyber-Physical System Research & Development Dept.,
Steel Res. Lab., JFE Steel

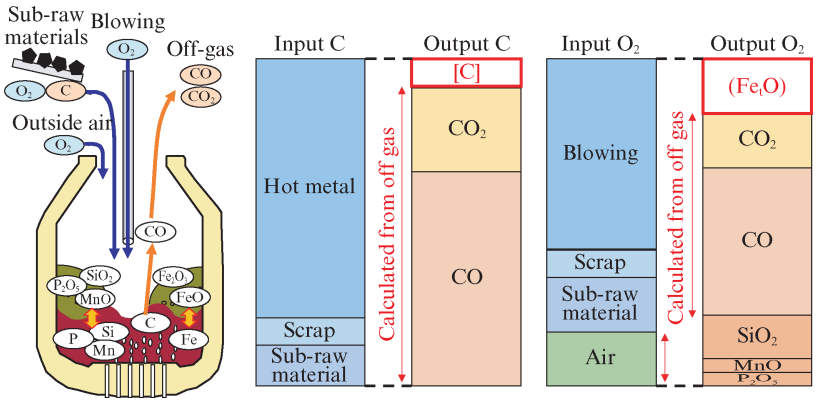

Fig. 2 Mass balance model

developed a high-accuracy model that enables continuous, real-time estimation of the internal state of the converter.

2. Conventional Converter State Estimation Model

Various models for estimation and prediction of the internal state of the converter have been proposed up to the present. For example, these include models for predicting the molten metal temperature, C concentration and P concentration at the end of blowing by utilizing data-driven models [1–6]. However, since the purpose of the present development is to estimate the converter internal state in real time during blowing, a mass balance model and chemical reaction model suitable for that purpose were adopted. First, this chapter explains these models.

2.1 Mass Balance Model

An overview of the mass balance model is shown in **Fig. 2**. In the converter, O_2 from the top-blown lance, sub-materials and outside air are introduced into the converter as inputs, and CO and CO_2 are discharged from the converter in the off-gas as outputs. In the mass balance model, the C concentration in the molten metal [C] and the amount of formed iron oxide in the slag [Fe_tO] are estimated based on a balance calculation for the C and O_2 inputs and outputs of the converter from the start of blowing up to the present time [7,8].

2.1.1 C balance calculation

The C charged into the converter consists of C in the hot metal, C in scrap and C in the sub-materials. C is discharged from the converter in the forms of CO and CO_2, which are formed in the decarburization reaction and discharged from the converter as off-gas. The C concentration in the molten metal $[C]_{mass}$ (10^{-2} kg/kg-metal) is calculated as shown in Eq. (1).

$$[C]_{mass} = C_{IN} - C_{OG} \quad \cdots\cdots (1)$$

Where, C_{IN} (10^{-2} kg/kg-metal) is calculated as shown in Eq. (2).

$$C_{IN} = \frac{\rho^{C}_{HM} W_{HM} + \sum_i \left(\rho_i^{Cscr} W_i^{scr}\right) + \sum_j \left(\rho_j^{Csub} W_j^{sub}\right)}{W_{ch}} \quad \cdots\cdots (2)$$

Where, ρ^{C}_{HM} (10^{-2} kg/kg-metal) is the C component ratio in the charged hot metal, ρ_i^{Cscr} (10^{-2} kg/kg-scrap) is the C component ratio in scrap brand i, ρ_j^{Csub} (10^{-2} kg/kg-sub) is the C component ratio in sub-material brand j, W_{HM} (kg) is the weight of the charged hot metal, W_i^{scr} (kg) is the weight of charged scrap brand i and W_i^{sub} (kg) is the weight of charged sub-material brand i. The weight of the molten metal W_{ch} (kg) is calculated as shown in Eq. (3).

$$W_{ch} = W_{HM} + \sum_i \frac{\rho_i^{Mscr} W_i^{scr}}{100} + \sum_j \frac{\rho_j^{Msub} W_j^{sub}}{100} \quad \cdots\cdots (3)$$

Where, ρ_i^{Mscr} (10^{-2} kg/kg-scrap) is the total component ratio of only the components (Fe, C, Si, Mn, P) of the molten metal in scrap brand i, and ρ_j^{Msub} (10^{-2} kg/kg-sub) is the total component ratio of only the above-mentioned components in sub-material brand j. The off-gas discharged from the converter, C_{OG} (10^{-2} kg/kg-metal), is calculated as shown in Eq. (4).

$$C_{OG} = \left(V_{CO}^{OG} + V_{CO_2}^{OG}\right) \times \frac{12 \times 100}{22.4} \quad \cdots\cdots (4)$$

Where, V_{CO}^{OG} (Nm^3/kg-metal) is the volume of CO in the off-gas per unit weight of molten metal, and V_{CO2}^{OG} (Nm^3/kg-metal) is the volume of CO_2 in the off-gas per unit weight of molten metal.

2.1.2 O_2 balance calculation

The O_2 inputs to the converter are the O_2 blown by the top-blown lance, the O_2 in scrap, the O_2 in sub-materials and the O_2 of the external air entrained in the off-gas. When the inert gas components (N_2, Ar) in the off-gas cannot be measured because a mass spectrometer, etc. has not been installed, the volume of oxygen in air entering from outside the converter, V_{O2}^{Air} (Nm^3/kg-metal), is calculated by Eq. (5).

$$V_{O_2}^{Air} = \frac{21}{79}\left(V^{OG} - V_{CO}^{OG} - V_{CO_2}^{OG} - V_{O_2}^{OG} - V^{BOT}\right) \quad \cdots\cdots (5)$$

Where, V^{OG} (Nm^3/kg-metal) is the volume of the off-gas per unit weight of molten metal, V_{O2}^{OG} (Nm^3/kg-metal) is the volume of O_2 in the off-gas per unit weight of molten metal and V^{BOT} (Nm^3/kg-metal) is the volume of bottom-blown gas per unit weight of molten metal.

The volume of oxygen consumed by oxidation of Si, V_{O2}^{SiO2} (Nm^3/kg-metal), the volume of oxygen consumed by oxidation of Mn, V_{O2}^{MnO} (Nm^3/kg-metal), and the volume of oxygen consumed by oxidation of P, V_{O2}^{P2O5} (Nm^3/kg-metal), are calculated by Eqs. (6) to (8).

$$V_{O_2}^{SiO_2} = \frac{\rho_{HM}^{Si} W_{HM} + \sum_i\left(\rho_i^{Siscr} W_i^{scr}\right) + \sum_j\left(\rho_j^{Sisub} W_j^{sub}\right)}{W_{ch}} \times\left(1 - \exp\left(-k_{Si} V_{O_2}^{BLW}\right)\right) \times \frac{22.4}{28.09 \times 100}$$

$$V_{O_2}^{MnO} = \frac{\rho_{HM}^{Mn} W_{HM} + \sum_i\left(\rho_i^{Mnscr} W_i^{scr}\right) + \sum_j\left(\rho_j^{Mnsub} W_j^{sub}\right)}{W_{ch}} \times\left(1 - \exp\left(-k_{Mn} V_{O_2}^{BLW}\right)\right) \times \frac{22.4}{54.94 \times 100} \times \frac{1}{2}$$

$$V_{O_2}^{P_2O_5} = \frac{\rho_{HM}^{P} W_{HM} + \sum_i\left(\rho_i^{Pscr} W_i^{scr}\right) + \sum_j\left(\rho_j^{Psub} W_j^{sub}\right)}{W_{ch}} \times\left(1 - \exp\left(-k_P V_{O_2}^{BLW}\right)\right) \times \frac{22.4}{30.97 \times 100} \times \frac{5}{2} \times \frac{1}{2}$$

$\cdots\cdots$ (6) — (8)

Where, $\rho^{Si}{}_{HM}$, $\rho^{Mn}{}_{HM}$ and $\rho^{P}{}_{HM}$ (10^{-2} kg/kg-metal) are the component ratios of Si, Mn and P in the charged hot metal, $\rho^{Siscr}{}_i$, $\rho^{Mnscr}{}_i$ and $\rho^{Pscr}{}_i$ (10^{-2} kg/kg-scrap) are the component ratios of Si, Mn and P in scrap brand i, $\rho^{Sisub}{}_j$, $\rho^{Mnsub}{}_j$ and $\rho^{Psub}{}_j$ (10^{-2} kg/kg-sub) are the component ratios of Si, Mn and P in sub-material brand j, k_{Si}, k_{Mn} and k_P are the oxidation rate constants of Si, Mn and P and V_{O2}^{BLW} (Nm^3/kg-metal) is the volume of O_2 in the top blown gas per unit weight of molten metal.

On the assumptions that the iron oxide formed by the oxidation reaction during blowing is all FeO, and the formed FeO is all absorbed into the slag, [9] $(FeO)_{mass}$ (kg/kg-metal) is calculated as shown in Eq. (9).

$$(FeO)_{mass} = \left(V_{O_2}^{IN} - V_{O_2}^{OUT}\right) \times \frac{1}{22.4} \times 2 \times 71.85 \quad \cdots\cdots (9)$$

V_{O2}^{IN} (Nm^3/kg-metal) is calculated as shown in Eq. (10).

$$V_{O_2}^{IN} = V_{O_2}^{BLW} + \sum_i\left(\rho_i^{Oscr} W_i^{scr}\right) + \sum_j\left(\rho_j^{Osub} W_j^{sub}\right) + V_{O_2}^{Air} \quad \cdots\cdots (10)$$

Where, ρ_i^{Oscr} (Nm^3/(kg-scrap·kg-metal) is the unit consumption per molten metal weight of the O_2 volume in scrap brand i and ρ_j^{Osub} (Nm^3/(kg-sub·kg-metal) is the unit consumption per molten metal weight of the O_2 volume in sub-material brand j.

V_{O2}^{OUT} (Nm^3/kg-metal) is calculated as shown in Eq. (11).

$$V_{O_2}^{OUT} = \frac{V_{CO}^{OG}}{2} + V_{CO_2}^{OG} + V_{O_2}^{OG} + V_{O_2}^{SiO_2} + V_{O_2}^{MnO} + V_{O_2}^{P_2O_5} \quad \cdots\cdots (11)$$

That is, the FeO concentration is calculated by Eq. (9), assuming that the remainder of the O_2 inputs to the converter, after excluding the fraction discharged from the converter or consumed in the oxidation reactions of other components, is consumed in oxidation of Fe.

2.1.3 Problems of mass balance model

In the mass balance model, estimation of the off-gas flow rate and the concentrations of the components (CO, CO_2) of the off-gas is extremely important. However, because converter off-gas is a high-temperature gas and contains a large amount of dust, errors frequently occur in measurements of these values. Thus, reduced accuracy of the mass balance model due to this type of measurement error was a problem, which made it difficult to maintain long-term operation of actual converters using only the mass balance model.

2.2 Chemical Reaction Model

A large number of chemical reaction models formulated on the basis of reaction kinetics models, equilibrium models, rule-based models, etc. have also been developed in contrast to the mass balance model described in the previous sections [10–15], but when the aim is real-time state estimation, a comparatively simple model with a low computational load is preferable.

Therefore, in this development, a simple model with a long history of use in estimation of [C] and (Fe_tO) was adopted.

2.2.1 Decarburization reaction model

As an example of a decarburization reaction model for estimation of [C], models [7,16] that describe decarburization oxygen efficiency have shown high accuracy in the end period of decarburization reaction and are also widely used in current operations. According to the model proposed by Fukumi et al., decarburization oxygen efficiency dC/dO_2 ((10^{-2} kg/kg-metal) / (Nm^3/kg-metal)), which indicates the amount of decarburization per unit of input oxygen, is calculated as shown in Eq. (12).

$$\frac{dC}{dO_2} = m_1\left\{1-\exp\left(\frac{C_L-[C]}{m_2W_{SLG}+m_3}\right)\right\} \quad \cdots\cdots\cdots \quad (12)$$

Where, C_L (10^{-2} kg/kg-metal) is a constant expressing the lower limit of the C concentration, W_{SLG} (kg/kg-metal) is the weight of slag per unit weight of molten metal, m_1 is a constant expressing the maximum value of decarburization oxygen efficiency, and m_2 and m_3 are constants. The C concentration $[C]_{mod}$ (10^{-2} kg/kg-metal) calculated by the decarburization reaction model is expressed by Eq. (13) by rearranging Eq. (12).

$$[C]_{mod} = C_L-\left(m_2W_{SLG}+m_3\right)ln\left\{1-\frac{\left(\frac{dC}{dO_2}\right)_{OG}}{m_1}\right\}$$

$$\cdots\cdots\cdots \quad (13)$$

Here, decarburization oxygen efficiency (dC/dO_2) ((10^{-2} kg/kg-metal) / (Nm^3/kg-metal)) can be calculated by Eq. (14) based on measured off-gas data.

$$\left(\frac{dC}{dO_2}\right)_{OG} = \frac{\left(V_{CO}^{OG}+V_{CO_2}^{OG}\right)_{temp}\times\frac{12\times100}{22.4}}{\left\{V_{O_2}^{BLW}+\sum_j\left(\rho_j^{Osub}W_j^{sub}\right)\right\}_{temp}} \quad \cdots\cdots \quad (14)$$

Where, $(\ )_{temp}$ expresses the amount of change in a recent predefined time period. Specifically, the numerator shows the total CO and CO_2 discharged from the converter in the recent time period, and the denominator shows the total top-blown oxygen blown into the converter and amount of oxygen in the charged sub-materials during that time period.

2.2.2 (Fe_tO) generation model

Formation of Fe_tO by oxidation of Fe in the molten metal can be modelled based on a reaction kinetics model[17]. Assuming that all the iron oxide formed by blowing is FeO, and this FeO is also absorbed in the slag[9], the formation reaction rate of FeO is calculated as shown in Eq. (15).

$$\frac{d(FeO)}{dt} = -\frac{k_SA}{V_S}\left\{(FeO)-(FeO)_e\right\}+eF_{O_2} \quad \cdots\cdots \quad (15)$$

Where, A (m^2) is the interfacial reaction area (bath surface area), V_S (m^3) is the slag volume, $(FeO)_e$ (10^{-2} kg/kg-slag) is the equilibrium iron oxide concentration in slag, e is a constant expressing the oxidation reaction efficiency of Fe with respect to the input oxygen blown by the top-blown lance and F_{O2} (Nm^3/s/kg-slag) is the oxygen flow rate by the top-blown lance per unit weight of slag. The iron oxide concentration in slag $(FeO)_{mod}$ (10^{-2} kg/kg-slag) calculated by the (Fe_tO) generation model from Eq. (15) is expressed by Eq. (16).

$$(FeO)_{mod} = \frac{1}{k_SA/V_S} \times\left[\left\{\frac{k_SA}{V_S}(FeO)_i-eF_{O_2}\right\}\exp\left(-\frac{k_SA}{V_S}t\right)+eF_{O_2}\right]$$

$$\cdots\cdots\cdots \quad (16)$$

Where, t (s) is time, and $(FeO)_i$ (10^{-2} kg/kg-metal) is the initial iron oxide concentration. k_s (m/s) is the mass transfer coefficient in slag, and is calculated as shown in Eq. (17).

$$k_S = B\exp\left(-\frac{155\,000}{RT}\right)\left(\varepsilon_{top}+\varepsilon_{bot}\right) \quad \cdots\cdots \quad (17)$$

Where, R (J/mol·K) is a gas constant (= 8.314), T (K) is temperature and B is a constant parameter.

ε_{top} (W/m^3) is the stirring power of the oxygen from the top-blown lance, and is calculated as shown in Eq. (18)[18].

$$\varepsilon_{top} = \frac{0.137\cos\theta}{V_m}\frac{Q_{O_2}{}^3N}{\lambda^2D^3h} \quad \cdots\cdots \quad (18)$$

Where, θ (rad) is the tilt angle of the top-blown lance, V_m (m^3) is the molten metal volume, Q_{O2} (Nm^3/s) is the oxygen flow rate of the top-blown lance, N is the molecular weight of the gas, λ is the number of holes of the top-blown lance nozzle, D (m) is the diameter of the top-blown lance nozzle and h (m) is the height of the top-blown lance.

ε_{bot} (W/m^3) is the stirring power of the bottom-blown gas, and is calculated as shown in Eq. (19)[19].

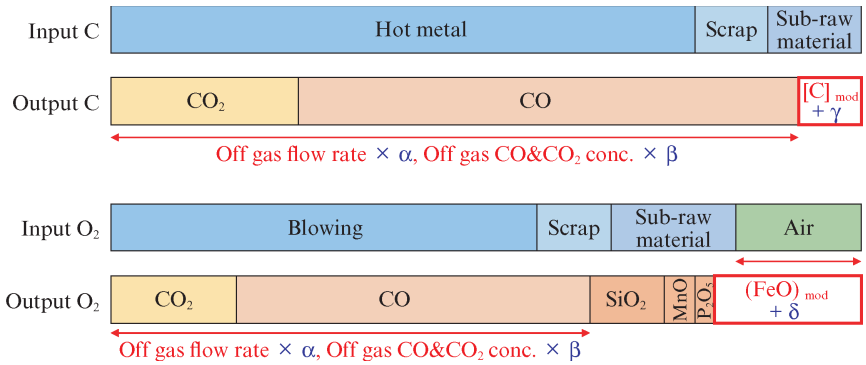

Fig. 3 Combination of mass balance models and chemical reaction models

$$\varepsilon_{bot} = \frac{372QT}{V_m}\left\{1 - \frac{273}{T} + \ln\left(1 + \frac{Z}{1.48}\right)\right\} \quad \cdots\cdots\cdots \quad (19)$$

Where, Q (Nm^3/s) is the flow rate of the bottom-blown gas, and Z (m) is the molten metal depth.

2.2.3 Problems of chemical reaction model

Using the chemical reaction model described above, highly accurate estimation is possible in laboratory experiments and actual converter experiments. However, in converters in actual operation, there are many unknown external disturbances which cannot be expressed by mathematical formulae, such as changes in the interfacial reaction area, nonuniform temperature distribution conditions, and changes in the equipment conditions. As one example of a measure to minimize decreased accuracy of the chemical reaction model caused by these factors, development of a model that can express the process in greater detail is conceivable. However, models of this type are generally complex, and require a larger number of measured data and tuning of many parameters, which easily increases the maintenance load of the model. For this reason, high-accuracy control in actual converter operation using only a chemical reaction model is not considered easy to be implemented.

3. Approach of this Research

3.1 Combination of Mass Balance Model and Chemical Reaction Model

JFE Steel developed a technique that reduces error by combining the mass balance model and the chemical reaction model.

First, we assumed that the measured values of the off-gas in the mass balance model and the calculated values obtained by the chemical reaction model include errors. Next, we introduced the following four correction parameters:

- Coefficient α for correction of the off-gas flow rate
- Coefficient β for correction of the CO and CO_2 concentrations in the off-gas
- Constant γ for correction of the estimated value of $[C]_{mod}$ in the decarburization reaction model
- Constant σ for correction of the estimated value $(FeO)_{mod}$ in the (Fe_tO) generation model

These correction parameters are determined so as to simultaneously minimize the error between the mass balance model and the chemical reaction model, making it possible to calculate the estimated values of the models so as to satisfy both model equations with high accuracy. **Figure 3** shows the mass balance relationships for C and O when the correction parameters were introduced.

3.2 Calculation of Correction Parameters

This section describes the method for determining the four newly-introduced correction parameters. In this method, the four correction parameters are determined so as to minimize the evaluation function J, which is shown in Eq. (20), and can simultaneously reduce the errors of the mass balance model and the chemical reaction model.

$$J = \frac{\left\{\left(C_{IN} - \alpha\beta C_{OG}\right) - \left(\left[C\right]_{mod} + \gamma\right)\right\}^2}{\sigma_1^{\,2}} + \frac{\left\{\left(V_{O_2}^{IN} - V_{O_2}^{OUT}\right) \times \frac{2 \times 71.85}{22.4} - \left(\left(FeO\right)_{mod} \times W_{SLG} \times \frac{1}{100} + \delta\right)\right\}^2}{\sigma_2^{\,2}} + \frac{\left(\alpha - \alpha_{ave}\right)^2}{\sigma_3^{\,2}} + \frac{\left(\beta - \beta_{ave}\right)^2}{\sigma_4^{\,2}} + \frac{\gamma^2}{\sigma_5^{\,2}} + \frac{\delta^2}{\sigma_6^{\,2}} \quad \cdots\cdots\cdots\cdots\cdots\cdots \quad (20)$$

Where, α_{ave} and β_{ave} are the reference constants for correction parameters α and β for the measured values of the off-gas, and σ_1 to σ_6 are weight parameters for each

of the terms of the evaluation function J.

V_{O2}^{Air}, which is included in V_{O2}^{IN} shown in Eq. (10), includes α and β, and is expressed as shown in Eq. (21).

$$V_{O_2}^{Air} = \frac{21}{79}\left\{\alpha\left(V^{OG} - V_{CO}^{OG} - V_{CO_2}^{OG} - V_{O_2}^{OG}\right) + 2\alpha(1-\beta)\frac{V_{CO}^{OG} + V_{CO_2}^{OG}}{2} - V^{BOT}\right\} \quad \cdots\cdots \quad (21)$$

Similarly, V_{O2}^{OUT} also includes α and β, and is expressed as shown in Eq. (22).

$$V_{O_2}^{OUT} = \alpha\beta\left(\frac{V_{CO}^{OG}}{2} + V_{CO_2}^{OG}\right) + \alpha V_{O_2}^{OG} + V_{O_2}^{SiO_2} + V_{O_2}^{MnO} + V_{O_2}^{P_2O_5} \quad \cdots\cdots \quad (22)$$

The first term of the evaluation function J expresses error between the C balance and the estimated value of $[C]_{mod}$ in the decarburization reaction model. The values of α, β and γ that achieve consistency between the C balance calculation and the decarburization reaction model can be determined by using this term.

The second term of the evaluation function J expresses the error between the O_2 balance and the estimated value $(FeO)_{mod}$ of the (Fe_tO) generation model, and makes it possible to determine α, β and δ so as to achieve consistency between the O_2 balance calculation and the (Fe_tO) generation model.

The third term and fourth term of the evaluation function J express the errors between α and β and the reference constants α_{ave} and β_{ave}. Addition of these terms in the equation has the effect of preventing significant deviations of α and β from the reference constants. The average values of the true values of the correction parameters α and β in multiple recent blowing operations were used in the reference constants α_{ave} and β_{ave}. It may be noted that the true values of the correction parameters α and β show the values obtained by calculating α and β where the C balance and the O_2 balance have been aligned by using the measured values of [C] and (FeO) obtained after blowing. If these terms continue to take the minimum values, this means that there are no large changes in α and β during blowing. In other words, these terms were added based on the assumption that trends in the errors of the off-gas flowmeter and the off-gas component analyzer do not change greatly in the short term.

The fifth and sixth terms of the evaluation function J are the absolute values of the correction constants γ and δ. Adding these two terms has the effect of preventing significant deviations of [C] and (Fe_tO) from the values calculated by the chemical reaction model.

By minimizing the evaluation function J comprising the four above-mentioned terms, it is possible to determine correction parameters that simultaneously achieve consistency in the mass balance model and the chemical reaction model, and as a result, estimated values appropriate for the respective model equations can be obtained. It should be noted that off-gas measurements are performed at a 1-second period, the parameters are determined each time the measurement results are obtained, and the parameters are updated in real time during blowing. In minimization of the evaluation function J in this research, we used sequential quadratic programming (SQP), which can be applied to both the nonlinear evaluation function and constraint condition.

3.3 Weight Parameter Switching Logic during Blowing

In this approach combining the mass balance model and a chemical reaction model, which model is to be prioritized can be adjusted by setting the weight parameters σ_1 to σ_6 of the evaluation function J. In the proposed method, the phase of the decarburization reaction is judged by using the estimated value of [C], the decarburization oxygen efficiency and other conditions, and automatic changing among σ_1 to σ_6 is possible. Changing the model to be prioritized by switching the weight parameters makes it possible to maintain high estimation accuracy at any point in time during blowing.

4. Evaluation of Accuracy of Proposed Model

Figure 4 shows an example of the results of an estimation of the amounts of [C] and FeO formed during one blowing operation using the proposed model. The changes in [C] and FeO formation were in good agreement with the following decarburization theory proposed by Fujii et al.[20]

- Blowing period I: In this period, the Si concentration in the molten steel is still extremely high, the high temperature of charged hot metal (molten pig iron) is decreased by contact with scrap, etc., and a bath temperature sufficient for the decarburization reaction to proceed fully has not been reached. As a result, the decarburization reaction is suppressed and the gradual increase in the decarburization rate starts in this period.
- Blowing period II: This is the period in which the bath temperature increases, the arrival rate of C at the reaction surface of the decarburization reaction is sufficiently large, and substantially 100% of the supplied oxygen is consumed in decarburization.

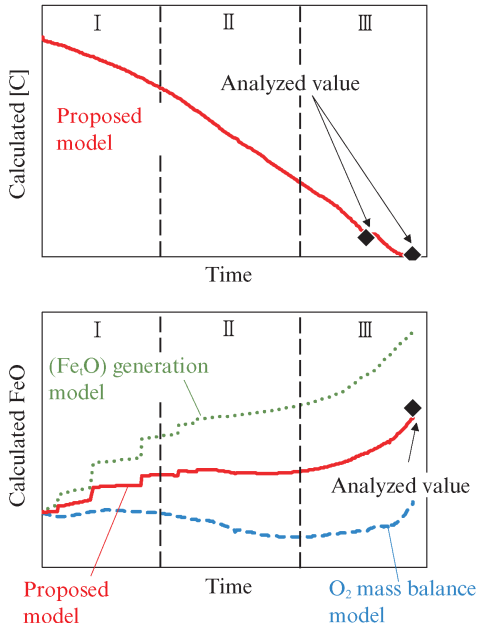

Fig. 4 Change in value of [C] and (FeO) calculated by proposed model during blowing

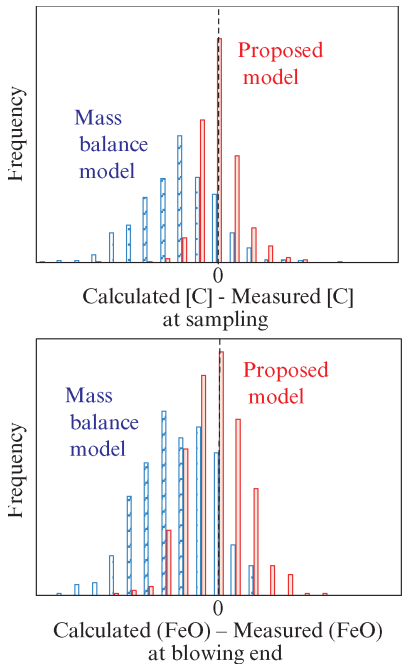

Fig. 5 Histograms of [C] and (FeO) errors between proposed model and measured value

Since the O_2 arrival rate at the reaction surface becomes the rate-determining step, the decarburization rate is determined by the oxygen blowing amount.

- Blowing period III: Decarburization proceeds, and the arrival rate of C at the reaction surface is slower than that of O_2 due to the decreased carbon concentration. Therefore, in this period, the C arrival rate at the reaction surface becomes the rate-determining step, and the decarburization rate decreases basically in proportion to the carbon concentration.

In blowing period I, the estimated value of [C] decreased slowly, while the estimated value of FeO increased. This is considered to be the result of the slow decarburization rate, and consumption of the excess oxygen for decarburization and oxidation of impurity metal components in the formation of FeO. In blowing period II, the rate of decrease in the estimated value of [C] increased, and the estimated value of FeO decreased slightly. This result is considered to be due to FeO reduction becoming more dominant than FeO formation, because decarburization efficiency has increased to almost 100% and all the supplied oxygen is used in the decarburization reaction. In blowing period III, the rate of decrease in the estimated value of [C] slowed, and the estimated value of FeO increased once again. This result is attributed to the decrease in decarburization reaction efficiency accompanying the decrease in [C], and the formation of FeO using the resulting excess oxygen.

Good agreement was obtained between the estimated values of [C] and the measured values by sampling performed two times, once during blowing and once after blowing. Furthermore, the estimated value of (FeO) showed an intermediate value between the values of the mass balance model and the chemical reaction model, and was in good agreement with the analysis results obtained by slag sampling after blowing.

Figure 5 shows the histograms of the error between the estimated values of [C] by the proposed model and the measured values obtained by sampling during blowing, and the histogram of the error between the estimated values of FeO calculated by the model and the analysis value after blowing. Here, the proposed model and the conventional mass balance model were calculated using the actual measured data from 490 charges, and the measured values and the estimated values were compared. The target charges were selected with no particular restrictions on the steel grade or other blowing conditions. Compared with the estimation results using only the conventional mass balance model, the average error in the estimation of [C] and FeO when using the proposed hybrid model was close to 0, the standard deviation of the estimation error of [C] decreased approximately 41%, and the standard deviation of the estimation error of FeO decreased approximately 21%.

5. Conclusion

JFE Steel developed a new model which makes it possible to estimate [C] and FeO in converter operation

in real time and with high accuracy. To reduce the estimation error caused by the measurement errors and unknown external disturbances, which are typical problems of the conventional technique, an approach in which the mass balance model and a chemical reaction model are combined, and the correction parameters of both models are determined successively during blowing, was established. In comparison with the conventional technique, the proposed model successfully achieved large reductions in the estimation errors of both [C] and FeO. Since this development has made it possible to estimate the internal state of the converter continuously and with high accuracy, as future work, the authors intend to promote dynamic control and automation of converter operation by building a cyber-physical system (CPS) utilizing this technique.

References

1) Han, M.; Liu, C. Endpoint prediction model for basic oxygen furnace steel-making based on membrane algorithm evolving extreme learning machine. Applied Soft Computing. 2014, vol. 19, p. 430–437.
2) Qi, L.; Liu, H.; Xiong, Q.; Chen, Z. Just-in-time-learning based prediction model of BOF endpoint carbon content and temperature via vMF mixture model and weighted extreme learning machine. Computers & Chemical Engineering. 2021, vol. 154, p. 107488.
3) Feng, L.; Zhao, C.; Li, Y.; Zhou, M.; Qiao, H.; Fu, C. Multichannel diffusion graph convolutional network for the prediction of endpoint composition in the converter steelmaking process. IEEE Transactions on Instrumentation and Measurement. 2021, vol. 70, p. 3000413.
4) Tang, L.; Liu, C.; Liu, J.; Wang, X. An estimation of distribution algorithm with resampling and local improvement for an operation optimization problem in steelmaking process. IEEE Transactions on Systems, Man, and Cybernetics: Systems. 2024, vol. 54, no. 3, p. 1346–1362.
5) Tomiyama, S.; Uchida, Y.; Mizuno, H.; Akiu, K.; Maeda, T. A novel control algorithm for dephosphorization in an LD converter. Journal of Process Control. 2015, vol. 25, p. 35–40.
6) He, F.; Zhang, L. Prediction model of end-point phosphorus content in BOF steelmaking process based on PCA and BP neural network. Journal of Process Control. 2018, vol. 66, p. 51–58.
7) Fukumi, J.; Taki, C.; Hatanaka, T.; Ogura, H. Development of refining control system in combined blowing converter based on exhaust gas information. Tetsu-to-Hagané. 1990, vol. 76, no. 11, p. 1956–1963.
8) Ogasawara, Y.; Miki, Y.; Uchida, Y.; Kikuchi, N. Development of high efficiency dephosphorization system in decarburization converter utilizing FetO dynamic control. Tetsu-to-Hagané. 2014, vol. 100, no. 8, p. 935–942.
9) Ban-ya, S.; Watanabe, T. Thermodynamics of FetO-P2O5 slags saturated with solid iron. Tetsu-to-Hagané. 1977, vol. 63, no. 12, p. 1809–1818.
10) Kattenbelt, C.; Roffel, B. Dynamic Modeling of the Main Blow in Basic Oxygen Steelmaking Using Measured Step Responses.-metallurgical and Materials Transactions B. 2008, vol. 39, p. 764–769.
11) Carlucci, A.P.; Ficarella, A.; Indiveri, G.; Presicce, P. An improved parameter identification schema for the dynamic model of LD converters. Journal of Process Control. 2015, vol. 31, p. 64–72.
12) Kadrolkar, A.; Andersson, N.Å.I.; Dogan, N. A dynamic flux dissolution model for oxygen steelmaking.-metallurgical and Materials Transactions B. 2017, vol. 48, p. 99–112.
13) Kruskopf, A.; Visuri, V. A Gibbs energy minimization approach for modeling of chemical reactions in a basic oxygen furnace.-metallurgical and Materials Transactions B. 2017, vol. 48, p. 3281–3300.
14) Song, D.; Tang, L.; Liu, C.; Wu, J.; Song, X. A novel operation optimization method based on mechanism analytics for the quality of molten steel in the BOF steelmaking process. IEEE Transactions on Automation Science and Engineering. 2023, vol. 20, no. 1, p. 218–232.
15) Liu, C.; Zheng, S.; Zhu, M. Variation in multiphase flow characteristics by single-flow post-combustion oxygen lance blowing in BOF steelmaking.-metallurgical and Materials Transactions B. 2023, vol. 54, p. 1245–1261.
16) Takawa, T.; Katayama, K.; Hoteiya, M.; Hirayama, N. The development of a mathematical model of endpoint control system for top and bottom blowing process in BOF. Tetsu-to-Hagané. 1987, vol. 73, no. 7, p. 836–843.
17) Matsui, A.; Nabeshima, S.; Matsuno, H.; Kikuchi, N.; Kishimoto, Y. Kinetics behavior of iron oxide formation under the condition of oxygen top blowing for dephosphorization of hot metal in the basic oxygen furnace. Tetsu-to-Hagané. 2009, vol. 95, no. 3, p. 207–216.
18) Kai, T.; Okuhira, K.; Hirai, M.; Murakami, S.; Sato, N. Influence of bath agitation intensity on metallurgical characteristics in top and bottom blown converter. Tetsu-to-Hagané. 1982, vol. 68, no. 14, p. 1946–1954.
19) Sundberg, Y. Mechanical stirring power in molten metal in ladles obtained by induction stirring and gas blowing. Scandinavian Journal of metallurgy. 1978, vol. 7, no. 2, p. 81–87.
20) Fujii, T.; Araki, T.; Marukawa, K. Consideration on decarburization reaction in an oxygen converter and possibility of the computing control on its basis. Tetsu-to-Hagané. 1967, vol. 53, no. 8, p. 973–982.
21) Kase, H.; Tomiyama, S.; Sato, S.; Iizuka, Y. Real-Time State Estimation Model for Converter Steelmaking. AISTech 2025-Proceedings of the Iron & Steel Technology Conference. 2025, p. 833–841.

This paper reproduces the paper listed as reference 21), which was written by the same lead author, with revisions of some expressions.